Molecular & Cellular Toxicology
https://doi.org/10.1007/s13273-026-00614-w

Circadian-dependent UV-B stress responses reveal differential antioxidant and photoprotective mechanisms in *Achyranthes japonica* microgreens

Ye Lin Kim[1] · Han-Sol Sim[1] · Jae Gil Yun[2] · Ki-Ho Son[1,2]

Received: 23 January 2026 / Revised: 23 January 2026 / Accepted: 4 March 2026

Abstract

Background Climate change increases exposure to ultraviolet-B (UV-B) radiation, which inhibits photosynthesis and causes DNA and cellular damage. While moderate UV-B exposure can enhance secondary metabolites, the impact of circadian timing on UV-B-induced toxicity and metabolic adaptation remains insufficiently explored, particularly in medicinal microgreens. *Achyranthes japonica*, a species with high pharmacological value, remains understudied at the microgreen stage.

Objective This study examined how short-term UV-B irradiation affects the growth, pigment accumulation, and antioxidant capacity of *A. japonica* microgreens across different circadian cycles. The normalized difference anthocyanin index, a biochemical response indicator that is non-destructive and induced by UV-B, was also evaluated.

Results Physiological and metabolic characteristics are affected by UV-B timing. During the day, UV-B promoted the accumulation of anthocyanin and phenolic compounds while preserving the efficiency of photosystem II and biomass. In contrast, nighttime UV-B exposure triggered photochemical damage but did not trigger pigment production. Continuous UV-B exposure increased anthocyanin levels but significantly reduced growth, consistent with the effects of cumulative stress. Antioxidant activity, measured by DPPH, ABTS, and FRAP, was highest with daytime treatment and lowest with nighttime exposure. A strong correlation was observed between NDAI and anthocyanin content and antioxidant capacity.

Conclusion The circadian time of UV-B exposure significantly affects the balance between protective metabolite production and growth stability maintenance. Short periods of UV-B during the day result in the most favorable balance of protective metabolite production and growth stability. These results highlight the value of microgreens as a model system for studying the timing of radiation-induced stress.

Keywords UV-B stress · *Achyranthes japonica* · Anthocyanin · Circadian regulation · Antioxidant defense · Photoprotection

Introduction

Ultraviolet-B (UV-B, 280–315 nm) is increasingly recognized as an important environmental toxin due to changes in solar radiation caused by atmospheric alterations resulting from climate change (Yin and Ulm 2017). The depletion of the stratospheric ozone layer raises concerns about increased UV-B exposure across ecosystems. This can lead to reduced photosynthetic performance, DNA damage induction, reactive oxygen species (ROS) production, and ultimately decreased crop productivity (Alexieva et al. 2001; Jansen 2002; Paul and Gwynn-Jones 2003). Understanding how plants perceive and respond to UV-B stress under future

✉ Ki-Ho Son
sonkh@gnu.ac.kr

Ye Lin Kim
dpflskol@naver.com

Han-Sol Sim
thfdl2828@naver.com

Jae Gil Yun
jgyun@gnu.ac.kr

[1] Department of GreenBio Science, Gyeongsang National University, Jinju 52828, Republic of Korea

[2] Division of Horticultural Science, Gyeongsang National University, Jinju 52828, Republic of Korea

Published online: 25 March 2026

environmental conditions is crucial given these toxicological effects. Simultaneously, evidence is growing that even environmentally relevant levels of UV-B can induce diverse physiological responses in plants, suggesting that UV radiation functions not only as a stressor but also as an informational signal within the surrounding environment (Paul and Gwynn-Jones 2003).

LED systems have advanced to enable controlled environment studies of UV-B signaling and toxicity by allowing precise spectral manipulation (Kusuma et al. 2020; Pinho et al. 2013). UV-B is perceived by a photoreceptor UVR8, which activates networks involved in defense and the biosynthesis of secondary metabolites, such as phenolics and flavonoids (Jenkins 2014; Zhang and Björn 2009). These act as antioxidants and UV screens, mitigating radiation-induced cellular injury. Consistent with this, UV-B exposure increases flavonoid levels in broccoli sprouts (Mewis et al. 2012) and both phenolic and flavonoid contents in basil microgreens (Dou et al. 2019). Microgreens are suitable systems for evaluating the biochemical and toxicological effects of light stress due to their rapid growth, heightened metabolic activity, and responsiveness to light environments (Brazaitytė et al. 2019; Sirtautas et al. 2012).

Circadian regulation is critical to plant stress response. The Earth's rotation generates diel cycles, and plants have endogenous circadian clocks that synchronize metabolism, ROS homeostasis, and stress signaling with these environmental rhythms (Jiménez et al. 2021). Similar UV-B stimuli can induce different physiological responses depending on the time of day at which they are perceived (Harmer 2009). In Arabidopsis, UV-B sensitivity is controlled by the circadian clock, with UVR8 signaling and phenylpropanoid metabolism exhibiting time-of-day specificity (Pérez-Llorca and Müller 2024; Takeuchi et al. 2014). Numerous secondary metabolite biosynthetic genes show circadian expression patterns associated with enhanced stress resilience (Doherty and Kay 2010). Anthocyanin biosynthesis follows a diel rhythm (Nguyen et al. 2015), and the transcription of ROS-related genes is strongly circadian-regulated, connecting oxidative stress management to temporal metabolic programming (Jiménez et al. 2021). These findings indicate that circadian gating modulates toxicity by shaping how sensitive plants are to UV-B exposure.

Anthocyanins are protective metabolites with strong antioxidant capacity that can mitigate UV-B-induced DNA damage (Chalker-Scott 1999; Takahashi et al. 1991). UV-B activates the UVR8–HY5–MYB regulatory axis to promote anthocyanin and flavonoid biosynthesis (Zhang et al. 2009), and anthocyanin-rich species, such as *Lycium ruthenicum,* show substantial pigment induction following UV-B treatment (Chen et al. 2024). Recently, imaging-based phenotyping tools are now effective methods for quantifying pigment responses to environmental stress. The normalized difference anthocyanin index (NDAI) correlates strongly with chemically quantified anthocyanin content and can also estimate leaf or canopy area (Kim and van Iersel 2023; Liu et al. 2024; Zhu et al. 2025), providing a scalable, non-destructive method for monitoring UV-B-induced oxidative and metabolic responses.

Achyranthes japonica is a traditionally valued medicinal herb containing triterpenoid saponins, polyphenols, and flavonoids with anti-inflammatory and antioxidant properties (Boo et al. 2010; Cho 2015; Jeong 2011). However, research has focused almost exclusively on mature tissues and extract-based pharmacology (Lee et al. 2012; Park et al. 2013), leaving the microgreen stage largely unexamined. However, no studies have examined the response of *A. japonica* microgreens to UV-B stress or the modulation of pigment accumulation, ROS-associated toxicity, or antioxidant defenses by temporal factors such as irradiation timing.

UV-B is becoming increasingly significant for the environment. It is also important for increasing the production of secondary metabolites. The effects of short-term UV-B exposure on the growth, anthocyanin accumulation, and antioxidant capacity of *A. japonica* microgreens were examined in this study. The study offers insights into the regulation of radiation-induced toxicity by evaluating UV-B responses under different circadian cycles. These findings suggest that *A. japonica* microgreens could serve as a plant-based model for environmental toxicology.

Materials and methods

Plant materials and cultivation conditions

Achyranthes japonica Nakai seeds were obtained from Aram Seeds Co., Ltd. (Seoul, Republic of Korea). For each treatment, 1 g of *A. japonica* seed was sown in a plastic tray ($31.5 \times 23 \times 7.5$ cm, $L \times W \times H$) filled with a commercial ginseng soil mix medium in a cultivation room. Germination was carried out in the dark for 4 days, and then the light was turned on. The cultivation room was maintained at 23 ± 2 °C, 50 ± 10% relative humidity, and 170 ± 15 µmol m^{-2} s^{-1} photosynthetic photon flux density (PPFD) using white LEDs over a 12 h photoperiod. The plants were irrigated with Hoagland's nutrient solution (pH 6.0, EC 1.0 dS m^{-1}).

Light treatment

Seventeen-day-old *A. japonica* microgreens were exposed to UV-B for one day prior to harvesting (day 18, Fig. 1A). UV-B LEDs (TUNP-AG120-UV-B100%-23W-PA, Japan Magnets, Suwa, Japan; peak wavelength at 308 nm) were used to provide a supplemental irradiance of 1.0 ± 0.1 W m^{-2} (Fig. 1B), and UV-B levels were measured using an

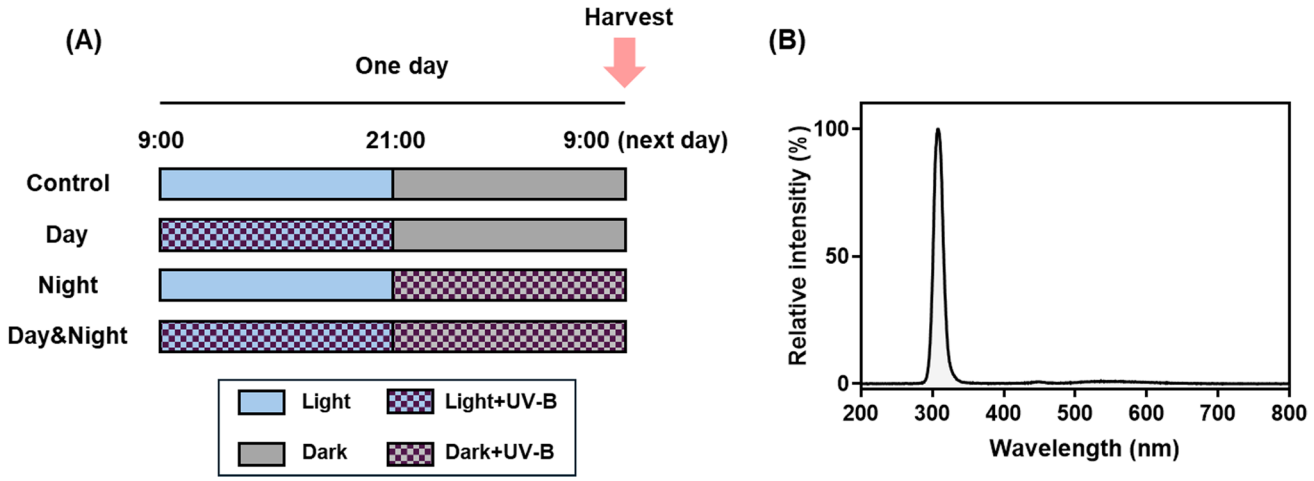

Fig. 1 Schematic illustration of UV-B treatment (**A**) and spectral distribution of UV-B LEDs (**B**) used in this study. The periods of UV-B irradiation were from 09:00 to 21:00 (Day UV-B), 21:00 to 09:00 (Night UV-B), and continuously for 24 h (Day and Night UV-B). The irradiance of UV-B light was maintained at 1.0 ± 0.1 W m^{-2} and applied one day before harvest

LP471-UVB sensor (Delta OHM, Padova, Italy; supplied by PCE Instruments S.L., Albacete, Spain). The treatments consisted of three UV-B exposure conditions: daytime exposure for 12 h with white LEDs on (Day), nighttime exposure for 12 h with white LEDs off (Night), and continuous exposure for 24 h combining both conditions (Day&Night). Control plants were not exposed to UV-B radiation.

Image-based analysis of anthocyanins

Top-down photographs of each experimental plant were captured using an iPhone 13 Pro Max camera immediately before harvesting following UV-B treatment. The RGB images were analyzed using an open-source Python program to calculate the normalized difference anthocyanin index (NDAI), a recently developed image-based index proposed by Kim and van Iersel (2023) for estimating anthocyanin concentration in plant tissues. The program automatically segmented the plant regions from the background and extracted the pixel intensities from the red (I_{red}) and green (I_{green}) channels of each image (Fig. 2).

The NDAI was calculated as follows:

$$NDAI = \frac{I_{red} - I_{green}}{I_{red} + I_{green}},$$

where I represents the pixel intensity (Kim and van Iersel 2023). Pixel-wise NDAI values were compiled into normalized histograms (area = 1), and kernel density estimation (KDE) was applied to visualize the distribution of anthocyanin-related signals.

Projected green cover

Projected green canopy cover (%) was determined from the same RGB images using a Python-based algorithm described by Patrignani and Ochsner (2015). Green pixels corresponding to photosynthetically active tissues were identified, and green cover was calculated as the proportion of green pixels relative to the total tray area.

Measurement of chlorophyll fluorescence, SPAD value, and anthocyanin content

The aerial parts of *A. japonica* seedlings were treated with different UV-B irradiation cycles for one day. Five plants were selected from each treatment group for biological replications. After 15 min of dark adaptation, the Fv/Fm values of true leaves were measured using a portable chlorophyll fluorometer (OS30P+, OPTI-SCIENCES. Inc., Hudson, NH, USA). Measurements were taken at 9:00 AM on the day of harvest, after UV-B treatment. SPAD values (SPAD-502Plus, Konica Minolta, Osaka, Japan) were measured using the largest true leaf. The anthocyanin content was measured using an ACM-200 Anthocyanin Content Meter (Opti-Sciences Inc., Hudson, NH, USA).

Determination of biomass and growth characteristics

Growth parameters were measured at 18 days after sowing. Fresh weight (FW), dry weight (DW), and relative water content (RWC) were measured on a tray basis, with each tray considered one experimental unit. Shoot height was measured in four randomly selected individual plants per

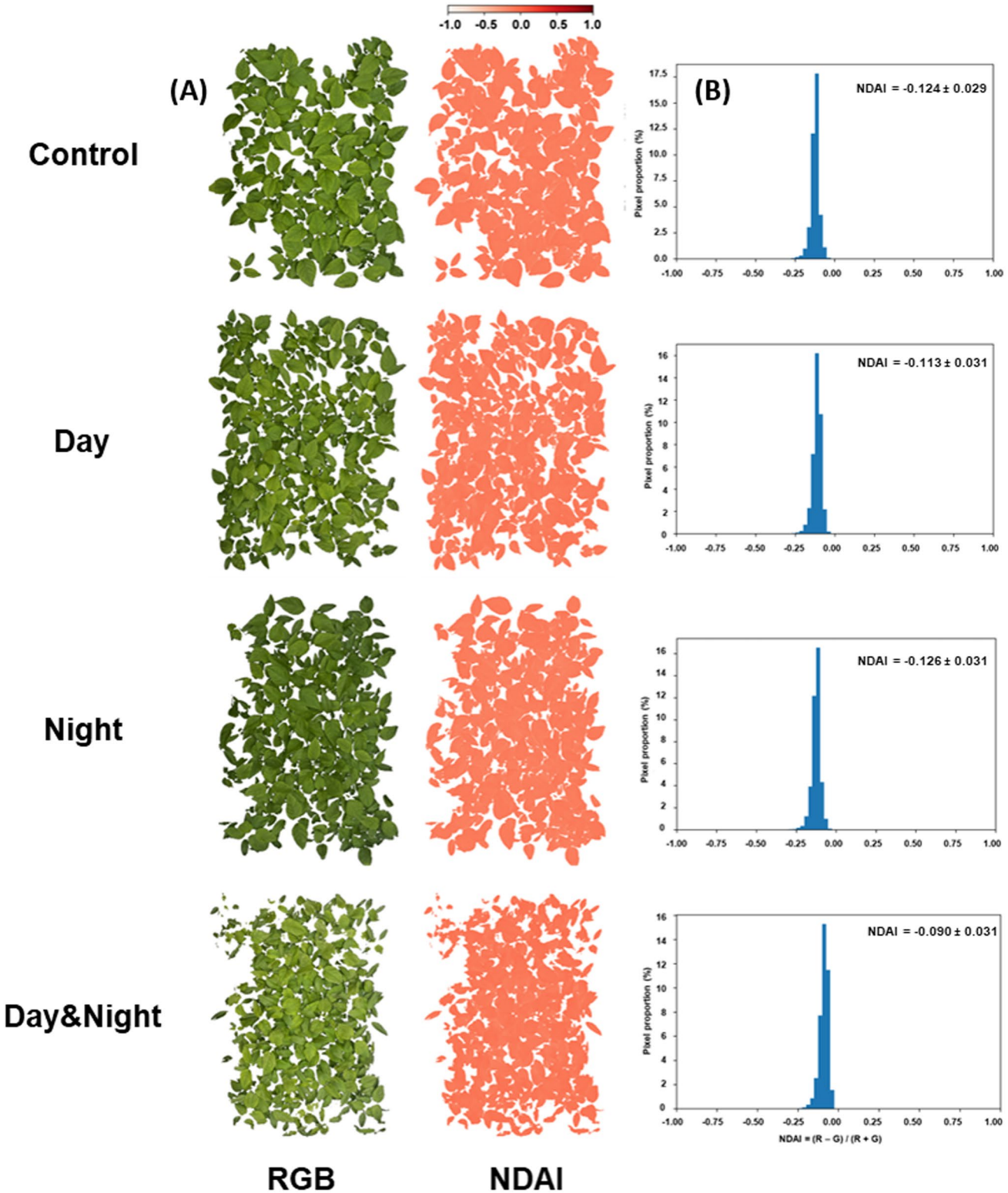

Fig. 2 **A** Canopy RGB (left) and normalized difference anthocyanin index (NDAI) images (right) of *Achyranthes japonica* microgreens, along with their corresponding histograms (**B**). The scale bar represents the NDAI values in these images. The numerical values within the histogram graphs represent the mean ± standard deviation of NDAI

tray. FW and DW were determined using a digital balance, and DW was obtained after oven-drying samples at 55 °C for 72 h. RWC was calculated based on the FW and DW values (Garnier et al. 1994). Compactness was calculated at the individual plant level as the ratio of DW (mg $plant^{-1}$) to shoot height (Moon et al. 2023):

$$RWC(\%) = FW(g) - DW(g)/FW(g) \times 100,$$

$$\text{Compactness (mg cm}^{-1}) = DW(\text{mg/plant})/\text{plant height(cm)}.$$

Bioactive compounds and antioxidant properties analysis

Total phenolic content (TPC) was determined using a slightly modified Folin–Denis method (Ainsworth and Gillespie 2007). TPC was expressed as milligrams of gallic acid equivalents (mg GAE g^{-1} DW). The total flavonoid content (TFC) was analyzed using a modified method described by Pękal and Pyrznska (2014). TFC was expressed as milligrams of quercetin equivalents (mg QE g^{-1} DW).

Antioxidant activity was assessed using DPPH, ABTS, and FRAP assays, with minor modifications as described by Lee et al. (2022). Dried powdered samples were extracted using 50% methanol and stirred for 14 h at room temperature. Absorbance was measured at 525 nm for DPPH, 732 nm for ABTS, and 590 nm for FRAP. Results were expressed as mg ascorbic acid equivalents or mg $FeSO_4$ equivalents g^{-1} DW.

Statistical analysis

Data were analyzed using one-way ANOVA followed by Tukey's post-hoc test ($p < 0.05$). Results are presented as mean ± SD. Statistical analyses and graphs were generated using GraphPad Prism (version 8.4), and correlation and heatmap analyses were performed using SRplot (https://www.bioinformatics.com.cn).

Results

Growth characteristics of *Achyranthes japonica* microgreens under different UV-B treatments

Changes in plant morphology are used to evaluate UV-B sensitivity (Zu et al. 2010). *Achyranthes japonica* (*A. japonica*) microgreens reacted differently to UV-B exposure (Fig. 3, Table 1). Fresh weight (FW) decreased with UV-B treatments, most notably with continuous Day&Night exposure. In contrast, dry weight (DW) did not differ significantly among treatments, suggesting that UV-B radiation affected fresh biomass and water-related parameters more strongly than total dry matter accumulation.

The relative water content (RWC) was highest in the control, slightly decreased under the Day and Night treatments. It was lowest under continuous UV-B exposure. There was no significant variation in plant height under the treatments. Compactness decreased most significantly under the Night UV-B treatment, indicating reduced tissue density and structural robustness. These morphological tendencies were consistent with Fig. 3, which shows that plants exposed to continuous UV-B irradiation had visibly reduced leaf area, decreased canopy density, and an overall dwarfed appearance.

Photosynthetic efficiency and pigment-related traits under different UV-B treatments

The photosynthetic efficiency and pigment-related traits of *A. japonica* microgreens were influenced by the timing of UV-B exposure (Fig. 4). The maximum quantum yield of PSII (Fv/Fm) remained comparable to that of the control under the Day UV-B treatment (Fig. 4A), indicating minimal photoinhibition. In contrast, the Night UV-B treatment reduced the Fv/Fm values, while daytime treatment showed the lowest values. Continuous UV-B exposure caused severe PSII damage.

Chlorophyll content, measured via SPAD values (Fig. 4B), was significantly reduced in the Day UV-B treatment compared to the control. However, SPAD values were similar to or higher than the control for both the Night and Day&Night treatment. Anthocyanin accumulation increased following UV-B exposure (Fig. 4C). Both Day and Night treatments produced moderate increases relative to the control, whereas the Day&Night treatment showed the highest anthocyanin index, indicating an enhancement of pigment biosynthesis under prolonged UV-B irradiation.

Canopy image analysis: green cover and normalized difference anthocyanin index (NDAI)

Canopy imaging analysis revealed clear differences in green cover and anthocyanin-related spectral traits depending on the timing of UV-B exposure (Fig. 5). Green cover (%) did not differ significantly among the Control, Day, and Night treatments, remaining at comparable levels (Fig. 5A). However, the Day&Night treatment exhibited a significant reduction in green cover, indicating a reduced canopy density under continuous UV-B exposure.

NDAI responses also varied according to the UV-B timing (Fig. 5B). The Day and Day&Night treatments showed significantly higher NDAI values than the Control, reflecting enhanced anthocyanin-related reflectance in the former. The Night treatment was not significantly different

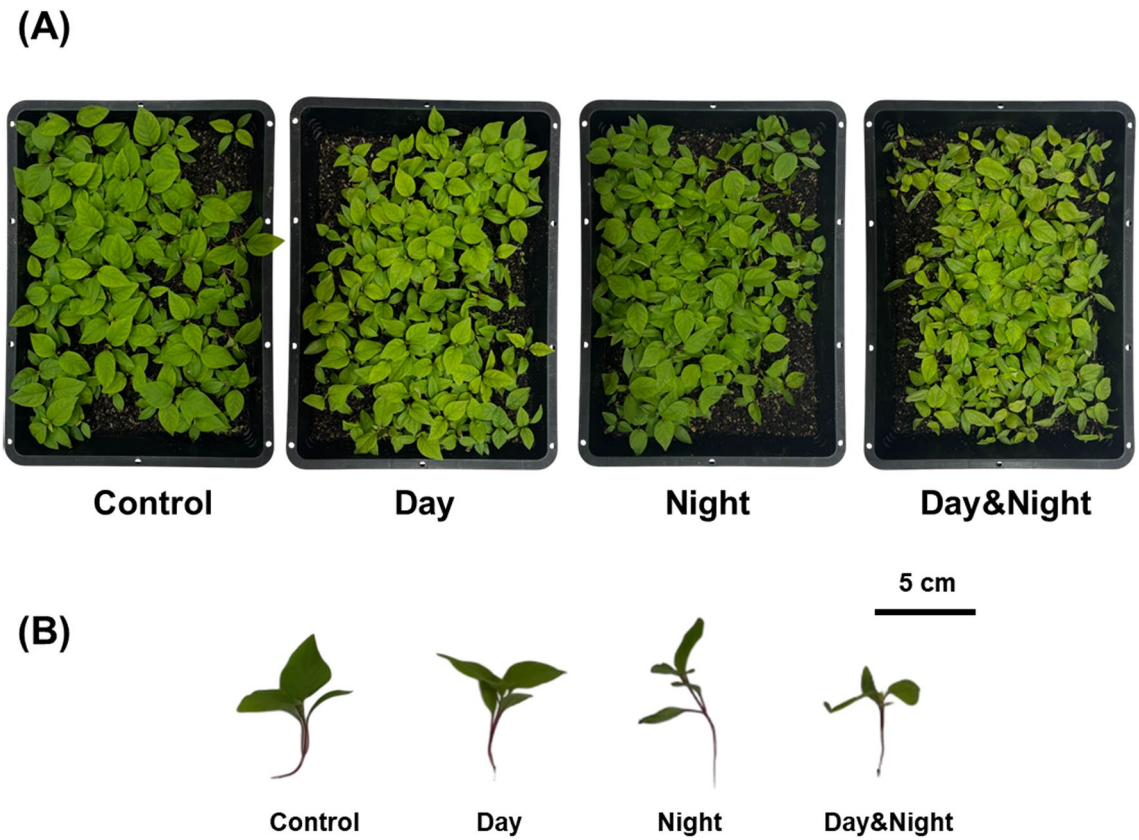

Fig. 3 *Achyranthes japonica* microgreen responses (**A**) to UV-B LEDs used in this study. The periods of UV-B irradiation were from 09:00 to 21:00 (Day UV-B), from 21:00 to 09:00 (Night UV-B), and continuously for 24 h (Day&Night UV-B). **B** Representative photographs of *Achyranthes japonica* microgreens after UV-B treatment

Table 1 Growth parameters of *Achyranthes japonica* Nakai microgreens under different UV-B treatment periods

Growth Parameter	Treatments			
	Control	Day	Night	Day & Night
FW (g)	16.22 ± 0.57[z] a[y]	14.32 ± 0.87 ab	15.19 ± 0.53 ab	12.64 ± 0.61 b
DW (g)	1.25 ± 0.04 a	1.25 ± 0.06 a	1.25 ± 0.05 a	1.20 ± 0.06 a
RWC (%)	92.32 ± 0.11 a	91.27 ± 0.25 b	91.82 ± 0.11 ab	90.54 ± 0.06 c
Plant height (cm)	4.03 ± 0.03 a	3.98 ± 0.08 a	3.88 ± 0.14 a	3.80 ± 0.05 a
Compactness (mg · cm^{-1})	5.50 ± 0.11 a	5.27 ± 0.28 a	3.76 ± 0.37 b	4.39 ± 0.3 ab

[z]Values represent mean ± S.D. ($n = 4$)

[y]Different letters indicate significant differences among treatments according to Tukey's HSD test ($p < 0.05$)

from the control. This suggests that nighttime UV-B alone was insufficient to induce strong canopy-level anthocyanin accumulation.

The kernel density estimation of the pixel-wise NDAI distribution further corroborated these findings (Fig. 5C). The Day and Day&Night curves shifted to higher NDAI values, suggesting increased anthocyanin accumulation through the canopy. Conversely, the Night treatment had a distribution almost identical to the control, a minimal anthocyanin response to UV-B exposure at night.

Secondary metabolites and antioxidant capacity under different UV-B treatments

A. japonica microgreens accumulated different levels of secondary metabolites and antioxidant capacity depending on when they were exposed to UV-B exposure (Fig. 6). The total phenolic content increased significantly under the Day and Day&Night treatments; both showed higher levels than the Control and Night treatments (Fig. 6A). The total flavonoid content showed an opposite pattern (Fig. 6B). The

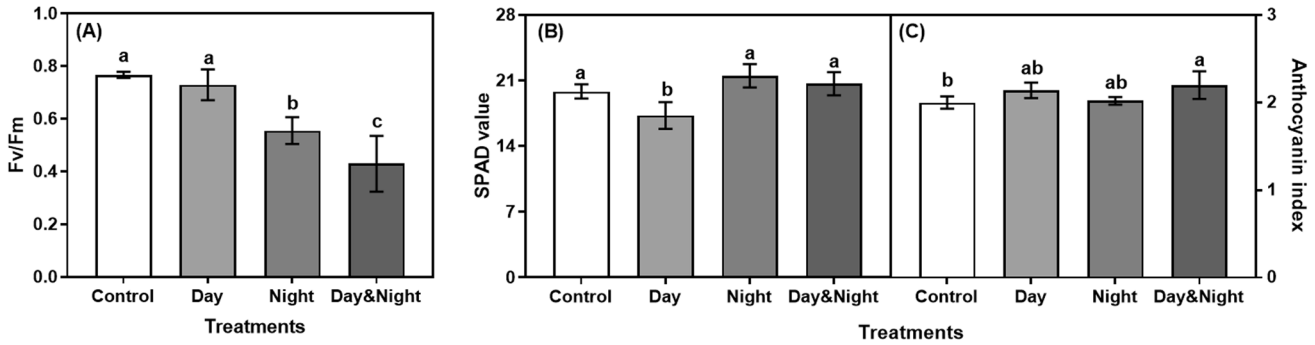

Fig. 4 Effects of different UV-B treatment periods on photosynthetic efficiency and pigment-related traits of *Achyranthes japonica* microgreens at harvest. **A** Maximum quantum efficiency of PSII (Fv/Fm). **B** Chlorophyll content measured as the SPAD value. **C** Anthocyanin content expressed as the anthocyanin cotent index, measured using an ACM-200 Anthocyanin Content Meter. Bars represent the mean ± SD ($n = 5$). Different letters above the bars indicate significant differences among treatments according to Tukey's HSD test ($p < 0.05$)

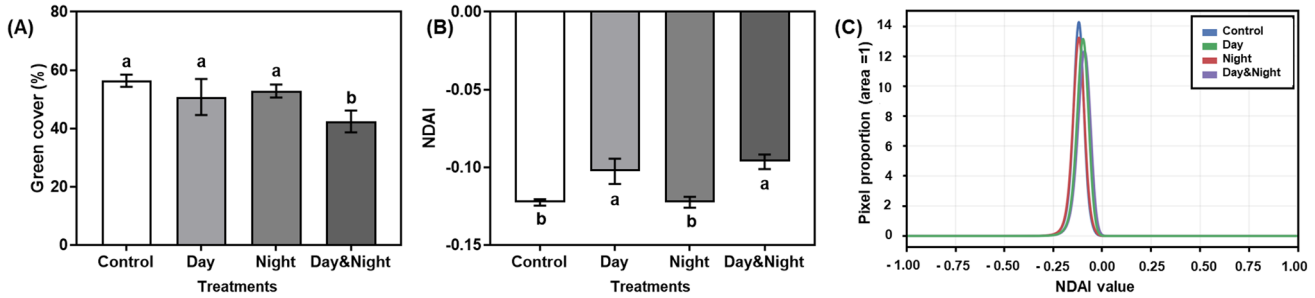

Fig. 5 Representative top-view canopy segmentation masks of control, Day-UV-B, Night-UV-B, and Day&Night-UV-B treatments at harvest. **A** Canopy cover (%) calculated as the proportion of green pixels per image. **B** Mean normalized difference anthocyanin index (NDAI) ± SD for each treatment, calculated from canopy RGB images using Python-based image analysis. **C** Kernel density estimation of the normalized difference anthocyanin index (NDAI) under different UV-B treatments. Bars represent the mean ± SD ($n = 4$). Different letters indicate significant differences at $p < 0.05$ (Tukey's HSD test)

Control and Day treatments maintained similar high levels. The Night and Day&Night treatments exhibited significantly reduced flavonoid accumulation. This indicates the suppression of flavonoid biosynthesis under nighttime or continuous UV-B exposure.

Antioxidant assays revealed treatment-dependent responses. DPPH radical-scavenging activity was highest in the Day treatment, followed by Day&Night, with the Control and Night treatments showing significantly lower activities (Fig. 6C). A similar tendency was observed for ABTS scavenging capacity: the Day treatment exhibited the strongest activity, the Night and Day&Night showed intermediate levels, and the Control showed the lowest values (Fig. 6D). Ferric-reducing antioxidant power (FRAP) was enhanced under Day and Day&Night UV-B treatments (Fig. 6E).

Correlation analysis among growth, physiological, and biochemical parameters

The correlation matrix showed different patterns of association among the growth parameters, pigment characteristics, and antioxidant activities of *A. japonica* microgreens that were exposed to different UV-B treatments (Fig. 7). There was a strong positive correlation ($r = 0.75$–1.00) among fresh weight, dry weight, plant height, and relative moisture content, suggesting these growth characteristics changed across the treatments. Compactness showed a moderate positive correlation with antioxidant activity such as FRAP and DPPH ($r = 0.44$–0.47). Strong intercorrelations were noted between the FRAP, ABTS, and DPPH antioxidant assays ($r = 0.80$–0.97). Furthermore, the total phenol content exhibited a strong positive correlation with antioxidant activity ($r = 0.50$–0.78). Anthocyanins demonstrated a moderate correlation with the ABTS and DPPH assays ($r = 0.74$–0.84). SPAD values were negatively correlated with phenols, flavonoids, and antioxidant properties, and showed weak correlations with growth parameters. Green cover showed a strong positive correlation ($r = 0.84$–0.99) with biomass-related traits and a very strong positive correlation ($r = 0.99$) with anthocyanins and NDAI. NDAI and total phenol content and antioxidant activity showed a strong positive correlation ($r = 0.74$–1.00), and a strong positive

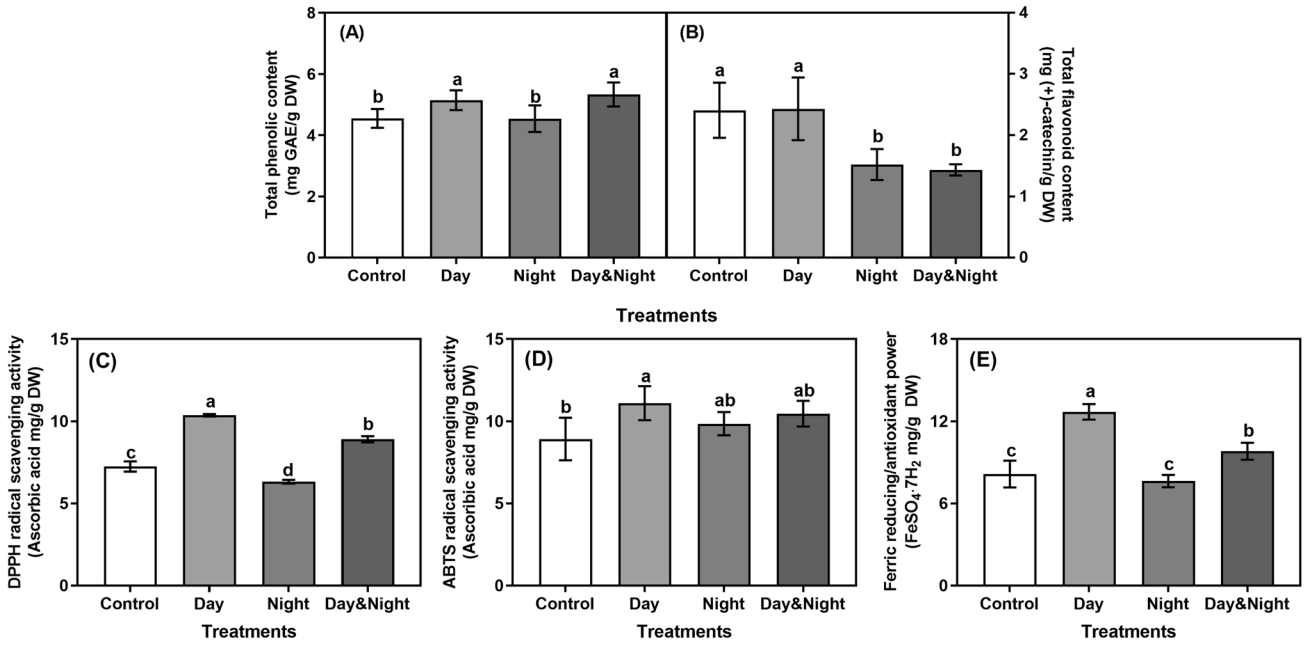

Fig. 6 Effects of different UV-B treatment periods on secondary metabolite accumulation and antioxidant activity of *Achyranthes japonica* microgreens at harvest. **A** Total phenolic content and **B** total flavonoid content of the extracts. **C** 2,2-diphenyl-1-picrylhydrazyl radical-scavenging activity (DPPH), **D** 2,2′-azino-bis(3-ethylbenzothiazoline-6-sulfonic acid) radical-scavenging activity (ABTS) and **E** Ferric-reducing antioxidant power (FRAP). Bars represent mean ± standard deviation ($n = 9$ for phenolic and flavonoid content; $n = 4$ for antioxidant assays). Different letters above the bars indicate significant differences among treatments according to Tukey's HSD test at $p < 0.05$

correlation ($r = 0.84$–0.99) with FW, DW, plant height, and percentage green cover.

Discussion

UV-B exposure affects *Achyranthes japonica* depending on the duration and timing of exposure. The fresh or dry weight was not significantly affected by short-term UV-B exposure during the day or night, suggesting that the dose was insufficient to cause irreversible oxidative or structural damage. This result is similar to what other studies have found about how leafy vegetables and microgreens can tolerate moderate UV-B radiation (Lee et al. 2021). In contrast, continuous 24-h UV-B irradiation resulted in growth inhibition, as indicated by reduced fresh weight and relative water content. Dry weight, however, remained unchanged. This pattern suggests that continuous UV-B exposure primarily affects water content rather than structural biomass accumulation. This response has also been observed in other species under UV-B stress (Bandurska et al. 2013). There was no significant difference in plant height between treatments, but a slight visual decrease in height upon UV-B irradiation was observed, consistent with a UV-B avoidance mechanism. These mechanisms include reduced elongation and minimized leaf expansion, which decrease incident UV-B absorption (Caldwell et al. 2007).

Compactness decreased under UV-B exposure at Night, emphasizing circadian regulation in modulating UV-B sensitivity. UV-B protective mechanisms, such as the UVR8–HY5 photomorphogenic cascade, exhibit reduced activity during the dark cycle (Takeuchi et al. 2014; Brown and Jenkins 2008). This circadian gating increases structural susceptibility to UV-B stress at night. This is likely explaining the more pronounced reduction in compactness compared to daytime exposure.

Canopy level responses reflected these leaf-scale effects and were measured. Green cover remained stable under short daytime and nighttime exposures but decreased under continuous UV-B, indicating growth inhibition. Similar reductions in canopy density were reported in potato plants under continuous UV-B stress (Zhang et al. 2025). Because UV-B increases ROS production and reduces leaf expansion (Chen et al. 2016), the decline in canopy density under continuous exposure reflects cumulative physiological stress.

Photosynthetic performance showed strong time-dependent effects. Daytime UV-B maintained Fv/Fm values within the normal range (Bartold and Kluczek 2024), suggesting effective photoprotective mechanisms when UV-B is perceived with visible light (Takeuchi et al. 2014). In contrast, nighttime and continuous UV-B exposure significantly

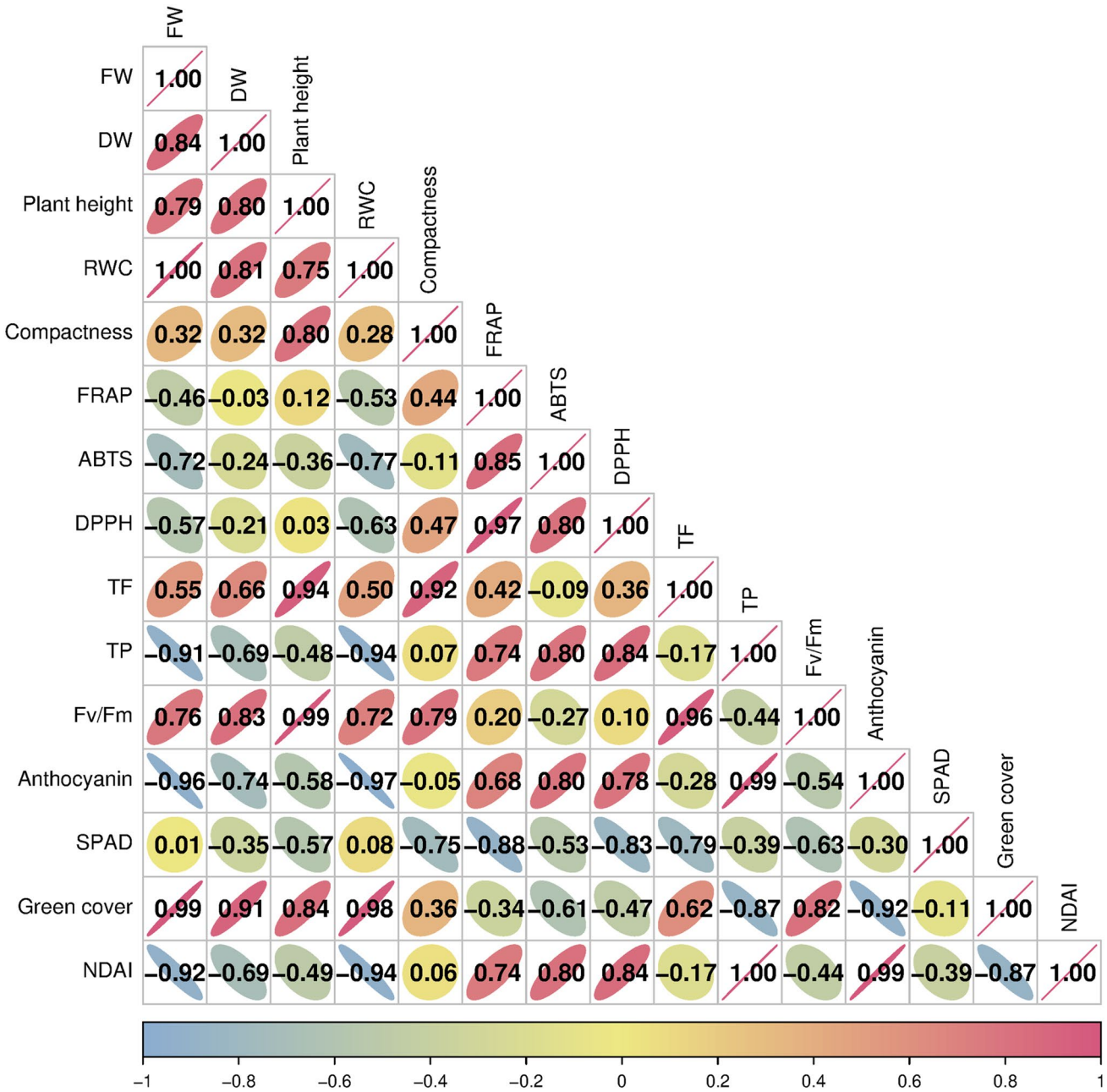

Fig. 7 Pearson's correlation matrix of growth, physiological, and biochemical parameters of *Achyranthes japonica* microgreens under different UV-B treatments. The correlation coefficients were calculated using the mean value of each parameter across all replicated measurements. Positive correlations are represented in red and negative correlations in blue, with the color intensity corresponding to the correlation strength

reduced Fv/Fm, consistent with the reduction in PSII efficiency observed in *Chenopodium album* following continuous UV-B irradiation (van Rensen et al. 2007). Earlier studies have reported that short-term UV-B exposure in the dark can markedly decrease chlorophyll fluorescence, reflecting the limited activation of protective mechanisms in the dark (Skórska 2000). Because downstream acclimation responses, such as HY5 induction (Brown and Jenkins 2008) and PSII repair, including D1 turnover (Bachmann et al. 2004), are strongly light dependent, minimal recovery from photodamage likely occurs during nighttime UV-B exposure, leading to increased PSII damage.

Chlorophyll content (SPAD) decreased only under daytime UV-B exposure. As chlorophyll breakdown is known to be accelerated under illumination (Maunders and Brown 1983) and increase with exposure to visible or ultraviolet

radiation (Sisson and Caldwell 1976), daytime UV-B likely directly stresses chlorophyll biosynthesis or stability. Despite the decrease in Fv/Fm, the SPAD reduction at night is absent, suggesting that photoinhibition can occur independently of changes in chlorophyll content.

UV-B exposure stimulated anthocyanin production in all treatments. The largest increases occurred under continuous UV-B exposure during the day. Studies show that anthocyanin biosynthesis is strongly light regulated and responds to UV-B in the presence of visible light (Tsurunaga et al. 2013). For instance, buckwheat sprouts accumulate negligible anthocyanin in the dark, but they quickly produce it when exposed to UV-B or visible light (Tsurunaga et al. 2013). The strong pigment enhancement observed here suggests a photoprotective role for anthocyanins in mitigating UV-B-induced oxidative damage.

Image-based NDAI further showed the time-dependence of pigment induction. NDAI increased in the Day and Day&Night treatments but not in the Night treatment, suggesting that pigment biosynthesis is strongly light dependent and requires the activation of light-sensitive transcriptional regulators, such as HY5 (Brown and Jenkins 2008; Yadav et al. 2020). Kernel density distributions confirmed higher NDAI values under daytime and continuous exposure, while nighttime UV-B was similar to the control. These results show that UV-B applied during active photoperception triggers anthocyanin induction at the canopy level.

Secondary metabolites also showed time-dependent responses to UV-B treatments. The total phenolic content increased under daytime and continuous UV-B exposure, consistent with their role as UV absorbers (Mosadegh et al. 2018) and with ROS-mediated induction through the phenylpropanoid pathway (Escobar et al. 2017). Conversely, flavonoid content decreased significantly during the nighttime and continuous exposure. Because flavonoid biosynthesis is strongly light dependent (Downey et al. 2004; Petrussa et al. 2013). Circadian modulation of UV-B signaling further suggests that effective flavonoid-based protection is initiated primarily during the photoperiod (Ferreyra et al. 2021).

Antioxidant activities (DPPH, ABTS, and FRAP) showed similar patterns. Daytime UV-B treatment resulted in the highest antioxidant activity levels, which is consistent with increased phenolic and flavonoid accumulation (Ghasemzadeh et al. 2016). Similar responses have been reported in wheat, tomato, and barley under UV-B exposure (Chen et al. 2019; Castagna et al. 2014; Wang et al. 2022), whereas nighttime exposure resulted in the weakest antioxidant response.

Correlation analysis showed a trade-off between growth and defensive measures, with growth traits positively associated with relative water content (Kaydan and Yagmur 2008), and defensive pigments positively associated with antioxidant activity, though negatively associated with growth parameters (González-Villagra et al. 2020; Song et al. 2023).

A radar chart summarized these responses (Figure S1) and shows that daytime UV-B exposure promotes balanced acclimation, while continuous UV-B exposure shifts plant metabolism into defense strategies at the disadvantage of growth. Overall, these findings emphasize the importance of timing in regulating UV-B-induced stress responses and defense strategies in microgreens.

This study investigated the physiological and metabolic responses of *Achyranthes japonica* microgreens to different UV-B exposure times. Daytime UV-B exposure activates photoprotective and antioxidant mechanisms, increasing anthocyanins and phenolic compounds without affecting PSII function. Nighttime and continuous UV-B exposure increased photochemical stress and decreased water status, demonstrating a circadian regulation of UV-B sensitivity. These results suggest that UV-B acts as a signaling molecule as an environmental stressor, and microgreens may serve as a model for assessing UV-B-induced physiological stress under changing environmental conditions.

Supplementary Information The online version contains supplementary material available at https://doi.org/10.1007/s13273-026-00614-w.

Author contributions Ye Lin Kim performed the research, analyzed the data, and wrote the manuscript. Han-Sol Sim conceived and designed the study. Jae Gil Yun and Ki-Ho Son reviewed and edited the manuscript. All the authors read and approved the final manuscript.

Funding This study was supported by the Research Sabbatical Grant for Research Professors from Gyeongsang National University in 2025.

Data availability The datasets generated during and analyzed during the current study are available from the corresponding author on reasonable request.

Declarations

Conflict of interest Ye Lin Kim declares that she has no conflict of interest. Han-Sol Sim declares that she has no conflict of interest. Jae Gil Yun declares that he has no conflict of interest. Ki-Ho Son declares that he has no conflict of interest.

Ethical approval This article does not contain any studies with human participants or animals performed by any of the authors.

References

Ainsworth EA, Gillespie KM (2007) Estimation of total phenolic content and other oxidation substrates in plant tissues using Folin-Ciocalteu reagent. Nat Protoc 2:875–877. https://doi.org/10.1038/nprot.2007.102

Alexieva V, Sergiev I, Mapelli S, Karanov E (2001) The effect of drought and ultraviolet radiation on growth and stress markers in pea and wheat. Plant Cell Environ 24(12):1337–1344. https://doi.org/10.1046/j.1365-3040.2001.00778.x

Bachmann KM, Ebbert V, Adams WW III, Verhoeven AS, Logan BA, Demmig-Adams B (2004) Effects of lincomycin on PSII efficiency, non-photochemical quenching, D1 protein and xanthophyll cycle during photoinhibition and recovery. Funct Plant Biol 31(8):803–813. https://doi.org/10.1071/FP04022

Bandurska H, Niedziela J, Chadzinikolau T (2013) Separate and combined responses to water deficit and UV-B radiation. Plant Sci 213:98–105. https://doi.org/10.1016/j.plantsci.2013.09.003

Bartold M, Kluczek M (2024) Estimating of chlorophyll fluorescence parameter Fv/Fm for plant stress detection at peatlands under Ramsar Convention with Sentinel-2 satellite imagery. Ecol Inform 81:102603. https://doi.org/10.1016/j.ecoinf.2024.102603

Boo KH, Lee D, Jeon G, Ko S, Cho SK, Kim, et al (2010) Distribution and biosynthesis of 20-hydroxyecdysone in plants of *Achyranthes japonica* Nakai. Biosci Biotechnol Biochem 74(11):2226–2231. https://doi.org/10.1271/bbb.100410

Brazaitytė A, Viršilė A, Samuolienė G, Vaštakaitė-Kairienė V, Jankauskienė J, Miliauskienė J et al (2019) Response of mustard microgreens to different wavelengths and durations of UV-A LEDs. Front Plant Sci 10:1153. https://doi.org/10.3389/fpls.2019.01153

Brown BA, Jenkins GI (2008) UV-B signaling pathways with different fluence-rate response profiles are distinguished in mature *Arabidopsis* leaf tissue by requirement for UVR8, HY5, and HYH. Plant Physiol 146(2):576. https://doi.org/10.1104/pp.107.108456

Caldwell MM, Bornman JF, Ballaré CL, Flint SD, Kulandaivelu G (2007) Terrestrial ecosystems, increased solar ultraviolet radiation, and interactions with other climate change factors. Photochem Photobiol Sci 6(3):252–266. https://doi.org/10.1039/B700019G

Castagna A, Dall'Asta C, Chiavaro E, Galaverna G, Ranieri A (2014) Effect of post-harvest UV-B irradiation on polyphenol profile and antioxidant activity in flesh and peel of tomato fruits. Food Bioprocess Technol 7(8):2241–2250. https://doi.org/10.1007/s11947-013-1214-5

Chalker-Scott L (1999) Environmental significance of anthocyanins in plant stress responses. Photochem Photobiol 70(1):1–9. https://doi.org/10.1111/j.1751-1097.1999.tb01944.x

Chen M, Huang Y, Liu G, Qin F, Yang S, Xu X (2016) Effects of enhanced UV-B radiation on morphology, physiology, biomass, leaf anatomy and ultrastructure in male and female mulberry (*Morus alba*) saplings. Environ Exp Bot 129:85–93. https://doi.org/10.1016/j.envexpbot.2016.03.006

Chen Z, Ma Y, Weng Y, Yang R, Gu Z, Wang P (2019) Effects of UV-B radiation on phenolic accumulation, antioxidant activity and physiological changes in wheat (*Triticum aestivum* L.) seedlings. Food Biosci 30:100409. https://doi.org/10.1016/j.fbio.2019.04.010

Chen S, Xu Y, Zhao W, Shi G, Wang S, He T (2024) UV-B irradiation promotes anthocyanin biosynthesis in the leaves of **Lycium ruthenicum* Murr*ay. PeerJ 12:e18199. https://doi.org/10.7717/peerj.18199

Cho KS (2015) Evaluation of **Achyranthes japonic*a* ethanol extraction on the inhibition effect of hyluronidase and lipoxygenase. J Life Sci 25(12):1370–1376. https://doi.org/10.5352/JLS.2015.25.12.1370

Doherty CJ, Kay SA (2010) Circadian control of global gene expression patterns. Annu Rev Genet 44:419–444. https://doi.org/10.1146/annurev-genet-102209-163432

Dou H, Niu G, Gu M (2019) Pre-harvest UV-B radiation and photosynthetic photon flux density interactively affect plant photosynthesis, growth, and secondary metabolites accumulation in basil (**Ocimum basilicu*m*) plants. Agronomy 9(8):434. https://doi.org/10.3390/agronomy9080434

Downey MO, Harvey JS, Robinson SP (2004) The effect of bunch shading on berry development and flavonoid accumulation in Shiraz grapes. AJGWR 10(1):55–73. https://doi.org/10.1111/j.1755-0238.2004.tb00008.x

Escobar AL, de Oliveira Silva FM, Acevedo P, Nunes-Nesi A, Alberdi M, Reyes-Díaz M (2017) Different levels of UV-B resistance in **Vaccinium corymbosu*m* cultivars reveal distinct backgrounds of phenylpropanoid metabolites. Plant Physiol Biochem 118:541–550. https://doi.org/10.1016/j.plaphy.2017.07.021

Ferreyra MLF, Serra P, Casati P (2021) Recent advances on the roles of flavonoids as plant protective molecules after UV and high light exposure. Physiol Plant 173(3):736–749. https://doi.org/10.1111/ppl.13543

Garnier E, Laurent G (1994) Leaf anatomy, specific mass and water content in congeneric annual and perennial grass species. New Phytol 128(4):725–736. https://doi.org/10.1111/j.1469-8137.1994.tb04036.x

Ghasemzadeh A, Ashkani S, Baghdadi A, Pazoki A, Jaafar HZ, Rahmat A (2016) Improvement in flavonoids and phenolic acids production and pharmaceutical quality of sweet basil (*Ocimum basilicum* L.) by ultraviolet-b irradiation. Molecules 21(9):1203. https://doi.org/10.3390/molecules21091203

González-Villagra J, Marjorie RD, Alberdi M, Acevedo P, Loyola R, Tighe-Neira R et al (2020) Solar UV irradiation effects on photosynthetic performance, biochemical markers, and gene expression in highbush blueberry (*Vaccinium corymbosum* L.) cultivars. Scientia Hortic 259:108816

Harmer SL (2009) The circadian system in higher plants. Annu Rev Plant Biol 60(1):357–377. https://doi.org/10.1146/annurev.arplant.043008.092054

Jansen MA (2002) Ultraviolet-B radiation effects on plants: induction of morphogenic responses. Physiol Plant 116(3):423–429. https://doi.org/10.1034/j.1399-3054.2002.1160319.x

Jenkins GI (2014) The UV-B photoreceptor UVR8: from structure to physiology. Plant Cell 26(1):21–37. https://doi.org/10.1105/tpc.113.119446

Jeong K-S (2011) A study on physicochemical properties of *Achyranthes japonica* and *Smilax china* extracts. J Korea Acad Ind Coop Soc 12(7):3317–3326. https://doi.org/10.5762/KAIS.2011.12.7.3317

Jiménez A, Sevilla F, Martí MC (2021) Reactive oxygen species homeostasis and circadian rhythms in plants. J Exp Bot 72(16):5825–5840. https://doi.org/10.1093/jxb/erab318

Kaydan D, Yagmur M (2008) Germination, seedling growth and relative water content of shoot in different seed sizes of triticale under osmotic stress of water and NaCl. Afr J Biotechnol 7(16):2862

Kim C, van Iersel MW (2023) Image-based phenotyping to estimate anthocyanin concentrations in lettuce. Front Plant Sci 14:1155722. https://doi.org/10.3389/fpls.2023.1155722

Kusuma P, Pattison PM, Bugbee B (2020) From physics to fixtures to food: current and potential LED efficacy. Hortic Res. https://doi.org/10.1038/s41438-020-0283-7

Lee SG, Lee EJ, Park WD, Kim JB, Kim EO, Choi SW (2012) Anti-inflammatory and anti-osteoarthritis effects of fermented *Achyranthes japonica* Nakai. J Ethnopharmacol 142(3):634–641. https://doi.org/10.1016/j.jep.2012.05.020

Lee JH, Shibata S, Goto E (2021) Time-course of changes in photosynthesis and secondary metabolites in canola (*Brassica napus*) under different UV-B irradiation levels in a plant factory with artificial light. Front Plant Sci 12:786555. https://doi.org/10.3389/fpls.2021.786555

Lee HY, Cho DY, Jang KJ, Lee JH, Jung JG, Kim MJ et al (2022) Changes of γ-aminobutyric acid, phytoestrogens, and biofunctional properties of the isoflavone-enriched soybean (*Glycine max*) leaves during solid lactic acid fermentation. Fermentation 8(10):525. https://doi.org/10.3390/fermentation8100525

Liu C, Yu H, Liu Y, Zhang L, Li D, Zhang, et al (2024) Prediction of anthocyanin content in purple-leaf lettuce based on spectral

features and optimized extreme learning machine algorithm. Agron 14(12):2915. https://doi.org/10.3390/agronomy14122915
Maunders MJ, Brown SB (1983) The effect of light on chlorophyll loss in senescing leaves of sycamore (*Acer pseudoplatanus* L.). Planta 158(4):309–311. https://doi.org/10.1007/BF00397332
Mewis I, Schreiner M, Nguyen CN, Krumbein A, Ulrichs C, Lohse M et al (2012) UV-B irradiation changes specifically the secondary metabolite profile in broccoli sprouts: induced signaling overlaps with defense response to biotic stressors. PCP 53(9):1546–1560. https://doi.org/10.1093/pcp/pcs096
Moon YH, Yang M, Woo UJ, Sim HS, Lee TY, Shin HR et al (2023) Evaluation of growth and photosynthetic rate of cucumber seedlings affected by far-red light using a semi-open chamber and imaging system. Horticulturae 9(1):98. https://doi.org/10.3390/horticulturae9010098
Mosadegh H, Trivellini A, Ferrante A, Lucchesini M, Vernieri P, Mensuali A (2018) Applications of UV-B lighting to enhance phenolic accumulation of sweet basil. Sci Hortic 229:107–116. https://doi.org/10.1016/j.scienta.2017.10.043
Nguyen NH, Jeong CY, Kang GH, Yoo SD, Hong SW, Lee H (2015) MYBD employed by HY 5 increases anthocyanin accumulation via repression of MYBL 2 in Arabidopsis. Plant J 84(6):1192–1205. https://doi.org/10.1111/tpj.13077
Park JH, Kang SN, Shin D, Hur IC, Kim IS, Jin SK (2013) Antioxidant activities of *Achyranthes japonica* Nakai extract and its application to the pork sausages. Asian-Australas J Anim Sci 26(2):287. https://doi.org/10.5713/ajas.2012.12438
Patrignani A, Ochsner TE (2015) Canopeo: a powerful new tool for measuring fractional green canopy cover. Agron J 107(6):2312–2320. https://doi.org/10.2134/agronj15.0150
Paul ND, Gwynn-Jones D (2003) Ecological roles of solar UV radiation: towards an integrated approach. Trends Ecol Evol 18(1):48–55
Pękal A, Pyrzynska K (2014) Evaluation of aluminium complexation reaction for flavonoid content assay. Food Anal Methods 7:1776–1782. https://doi.org/10.1007/s12161-014-9814-x
Pérez-Llorca M, Müller M (2024) Unlocking nature's rhythms: insights into secondary metabolite modulation by the circadian clock. Int J Mol Sci 25(13):7308. https://doi.org/10.3390/ijms25137308
Petrussa E, Braidot E, Zancani M, Peresson C, Bertolini A, Patui S et al (2013) Plant flavonoids—biosynthesis, transport and involvement in stress responses. Int J Mol Sci 14(7):14950–14973. https://doi.org/10.3390/ijms140714950
Pinho P, Hytönen T, Rantanen M, Elomaa P, Halonen L (2013) Dynamic control of supplemental lighting intensity in a greenhouse environment. Light Res Technol 45:295–304. https://doi.org/10.1177/1477153512444064
Sirtautas R, Sakalauskienė S, Jankauskienė J, Duchovskis P, Novičkovas A, Samuolienė G et al (2012) The impact of supplementary short-term red LED lighting on the antioxidant properties of microgreens. In: VII international symposium on light in horticultural systems, vol 956, pp 649–656. https://doi.org/10.17660/ActaHortic.2012.956.78
Sisson WB, Caldwell MM (1976) Photosynthesis, dark respiration, and growth of *Rumex patientia* L. exposed to ultraviolet irradiance (288 to 315 nanometers) simulating a reduced atmospheric ozone column. Plant Physiol 58(4):563–568. https://doi.org/10.1104/pp.58.4.563
Skórska E (2000) Comparison of responses of bean, pea and rape plants to UV-B radiation in darkness and in light. Acta Physiol Plant 22(2):163–169. https://doi.org/10.1007/s11738-000-0072-8
Song Y, Ma B, Guo Q, Zhou L, Zhou X, Ming Z et al (2023) MYB pathways that regulate UV-B-induced anthocyanin biosynthesis in blueberry (*Vaccinium corymbosum*). Front Plant Sci 14:1125382. https://doi.org/10.3389/fpls.2023.1125382
Takahashi A, Takeda K, Ohnishi T (1991) Light-induced anthocyanin reduces the extent of damage to DNA in UV-irradiated *Centaurea cyanus* cells in culture. Plant Cell Physiol 32(4):541–547. https://doi.org/10.1093/oxfordjournals.pcp.a078113
Takeuchi T, Newton L, Burkhardt A, Mason S, Farré EM (2014) Light and the circadian clock mediate time-specific changes in sensitivity to UV-B stress under light/dark cycles. J Exp Bot 65(20):6003–6012. https://doi.org/10.1093/jxb/eru339
Tsurunaga Y, Takahashi T, Katsube T, Kudo A, Kuramitsu O, Ishiwata M et al (2013) Effects of UV-B irradiation on the levels of anthocyanin, rutin and radical scavenging activity of buckwheat sprouts. Food Chem 141(1):552–556. https://doi.org/10.1016/j.foodchem.2013.03.032
van Rensen JJ, Vredenberg WJ, Rodrigues GC (2007) Time sequence of the damage to the acceptor and donor sides of photosystem II by UV-B radiation as evaluated by chlorophyll a fluorescence. Photosynth Res 94(2):291–297. https://doi.org/10.1007/s11120-007-9177-x
Wang M, Leng C, Zhu Y, Wang P, Gu Z, Yang R (2022) UV-B treatment enhances phenolic acids accumulation and antioxidant capacity of barley seedlings. LWT 153:112445. https://doi.org/10.1016/j.lwt.2021.112445
Yadav A, Singh D, Lingwan M, Yadukrishnan P, Masakapalli SK, Datta S (2020) Light signaling and UV-B-mediated plant growth regulation. J Integr Plant Biol 62(9):1270–1292. https://doi.org/10.1111/jipb.12932
Yin R, Ulm R (2017) How plants cope with UV-B: from perception to response. Curr Opin Plant Biol 37:42–48. https://doi.org/10.1016/j.pbi.2017.03.013
Zhang WJ, Björn LO (2009) The effect of ultraviolet radiation on the accumulation of medicinal compounds in plants. Fitoterapia 80(4):207–218. https://doi.org/10.1016/j.fitote.2009.02.006
Zhang X, He J, Guo Z, Li Y, Guo H (2025) StHY5 regulates potato plant morphology to accommodate UV-B radiation. Plant Physiol Biochem. https://doi.org/10.1016/j.plaphy.2025.110376
Zhu Y, Patil BS, Zhen S (2025) From ultraviolet-B to red photons: effects of end-of-production supplemental light on anthocyanins, phenolics, ascorbic acid, and biomass production in red leaf lettuce. PLoS ONE 20(7):e0328303. https://doi.org/10.1371/journal.pone.0328303
Zu YG, Pang HH, Yu JH, Li DW, Wei XX, Gao YX et al (2010) Responses in the morphology, physiology and biochemistry of *Taxus chinensis* var. *mairei* grown under supplementary UV-B radiation. J Photochem Photobiol B Biol 98(2):152–158. https://doi.org/10.1016/j.jphotobiol.2009.12.001